Hexasulphur Tetranitrogen Dichloride, S₆N₄Cl₂ : Crystal Growth and Crystal Structure †

Ronald W. H. Small
Department of Chemistry, University of Lancaster, Bailrigg, Lancaster LA1 4YA
Arthur J. Banister * **and Zdenek V. Hauptman**
Department of Chemistry, University of Durham, South Road, Durham DH1 3LE

Crystals of the title compound (commonly called thiodithiazyl chloride) are orthorhombic, space group *Pbca*, with $a = 7.88(1)$, $b = 14.46(1)$, $c = 8.19(1)$ Å, and $Z = 4$. The structure was refined to $R = 0.031$ using 563 (of the 792 unique) measured intensities for which $I > 3\sigma(I)$. The dimeric cation contains two centrosymmetric planar S_3N_2 rings in a chair (*trans*) conformation. Distances are $S(1)-N(1)$ 1.563(5), $N(1)-S(3)$ 1.618(4), $S(2)-S(3)$ 2.131(2), $S(2)-S(3')$ 2.916(2), and $Cl-S(2,3)$ 2.842(2), 2.858(2) Å. The dihedral angle between the S_3N_2 ring plane and the central S_4 ring is 110.4(3) °. Crystals of $S_6N_4Cl_2$ were grown by three different methods based on (*i*) a reversible temperature-dependent ring expansion–contraction ($S_6N_4Cl_2 \longleftrightarrow S_4N_3Cl$) equilibrium in SO_2-SOCl_2 mixtures, (*ii*) a complex chemical transport (vapour–liquid–solid) in a sealed tube containing (initially) $S_3N_2Cl_2$ and liquid SO_2, and (*iii*) a controlled slow reaction of $S_3N_2Cl_2$ with liquid SO_2. The last method is a particularly convenient laboratory synthesis of pure $S_6N_4Cl_2$. Solid $S_6N_4Cl_2$ shows a strong e.s.r. signal which is independent of temperature (in the range −139 to +22 °C), indicating the presence of a little monomer.

The compound with empirical formula S_3N_2Cl, commonly called thiodithiazyl chloride, is one of the few simple sulphur–nitrogen halides of hitherto unknown structure, and several structural types have been predicted.[1-3] The dark green (almost black) and metallic appearance of S_3N_2Cl, and its lack of solubility in virtually all solvents (except when accompanied by decomposition), indicated a polymeric structure.[3] The absence of a chlorine n.q.r. signal [1] pointed to an ionic lattice and this was reinforced by the isolation of ionic derivatives (with $ClS_2O_6^-$,[1] $S_2O_2F^-$,[4] or SO_3F^-ions [4]). In these salts, the cation is dimeric with two delocalised S_3N_2 rings in a *trans* conformation (I); however, isoelectronic phenyldithiadiazole contains two *cis* (eclipsed) rings, structure (II). Monomeric $S_3N_2^+$ salts have also been prepared.[4-6]

Since doubt remained as to the structure of S_3N_2Cl (and also since a small anion facilitates more compact structures), we studied methods of synthesis and crystal growth and carried out an *X*-ray diffraction analysis which showed that the chloride is dimeric. The reaction between $S_3N_2Cl_2$ and liquid SO_2 is a simple and convenient method of preparation and gives pure crystalline $S_6N_4Cl_2$. We also describe the preparation of a carmine red form of $S_6N_4Cl_2$.

Experimental

Manipulations of solids were carried out in a Vacuum Atmospheres Corporation glove box (HE43-2). I.r. spectra were obtained using a Perkin-Elmer grating spectrophotometer (model 577) and Raman spectra were recorded using a Cary 82 spectrometer with green (514.5 nm) exciting line. Haake refrigerated bath circulators (type F2-C, range −15 to +90 °C) were used to provide circulating water with a steady temperature or a controlled temperature gradient (as in the purification of $S_6N_4Cl_2$).

After combustion of samples in oxygen, nitrogen analysis was by the micro-Kjeldahl method, sulphur was determined as $BaSO_4$ and chlorine by potentiometric titration as AgCl.

† *Supplementary data available* (No. SUP 23912, 9 pp.): structure factors, thermal parameters, projection of the unit cell. See Instructions for Authors, *J. Chem. Soc., Dalton Trans.*, 1984, Issue 1, pp. xvii—xix.

(I)   (II)
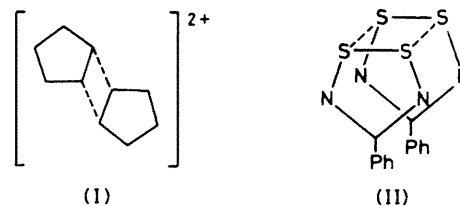
Thionyl chloride was purified by fractional distillation from triphenyl phosphite.[7] Liquid SO_2 was dried over P_4O_{10}, distilled and stored over CaH_2; it was transferred to reaction vessels *via* a Monel metal vacuum line. $S_6N_4Cl_2$ was obtained from $S_3N_2Cl_2$ (prepared from NH_4Cl and S_2Cl_2) [8] either by heating [9] or by dechlorination with SO_2.[10]

Purification of Crude $S_6N_4Cl_2$.—Continuous extraction with liquid SO_2 (15 min at *ca.* 2 cm³ SO_2 per min) in a sealed extractor, shown in Figure 1 (with evaporator flask at 25 °C and water-cooled extraction compartment at 10 °C), proved an efficient means of purification. After placing $S_6N_4Cl_2$ on the frit and evacuation, dry SO_2 was condensed in. Impurities (largely S_4N_3Cl which produced a yellow solution) were extracted until the SO_2 refluxing through the frit was colourless. Extraction for several hours gave tiny (*ca.* 0.05 mm wide) platelets of $S_6N_4Cl_2$ in the filtrate. During further extraction these crystals decomposed to S_4N_3Cl; nevertheless, above the SO_2 surface, tiny crystals of $S_6N_4Cl_2$ remained and grew on the flask walls (cooler due to rapid evaporation of SO_2), hence indicating that the reaction in the bulk SO_2 solution ($S_6N_4Cl_2$ $\longrightarrow S_4N_3Cl$) was reversed at the lower temperatures of the glass surface. We therefore interpret the reported [11] slight solubility of $S_6N_4Cl_2$ in liquid SO_2 as being largely due to chemical reaction. A similar conversion to $S_6N_4Cl_2$ occurs when solutions of S_4N_3Cl in $SOCl_2$ are cooled to *ca.* −5 °C; S_4N_3Cl is regenerated on warming.[12]

This facile temperature-dependent and reversible interconversion $S_6N_4Cl_2 \longleftrightarrow S_4N_3Cl$ was exploited in the preparation of small crystals of $S_6N_4Cl_2$ (methods 1 and 2).

Method 1. Sealed Tube Recrystallisations of $S_6N_4Cl_2$ *Suspended in* SO_2-SOCl_2.—Five sealed Pyrex ampoules
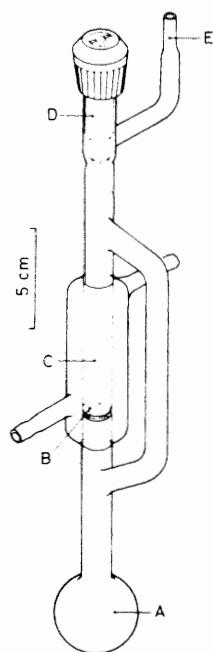
Figure 1. Sealed extractor for liquid SO_2: A, evaporator flask; B, sintered filter (porosity grade 3); C, water jacketted extraction compartment; D, Rotaflo valve (TF6/18); E, $\frac{1}{4}$-inch o.d. connection to Swagelok-type metal union

Figure 2. E.s.r. powder spectrum of $S_6N_4Cl_2$ ($G = 10^{-4}$ T)

Cooling to *ca.* $-60\,°C$ caused the signal to disappear. Interestingly, the yellow colour of the solution at room temperature changed sharply to deep purple at *ca.* $-60\,°C$. The change was reversible. In contrast, the solid $S_6N_4Cl_2$ gave a strong e.s.r. signal (shown in Figure 2) that is characteristic of powders and is temperature independent between -139 and $+22\,°C$. A more detailed assessment of the e.s.r. spectra is in progress.

Method 2. Growth of $S_6N_4Cl_2$ *Crystals by Vapour Transport during* $S_3N_2Cl_2$–SO_2 *Reaction.*—A sealed Pyrex tube (volume 12 cm³) containing $S_3N_2Cl_2$ (1.3 g) and liquid SO_2 (5.5 cm³) was placed horizontally in a sharp temperature gradient [$+35$ to $-8\,°C$, Figure 3(a)]. After one week most of the initial $S_3N_2Cl_2$ was converted to $S_6N_4Cl_2$ and well formed platelets [Figure 3(b)] grew on the upper wall (well above the SO_2 level) at *ca.* $5\,°C$ in the zone of steepest temperature gradient (*ca.* $15\,°C\ cm^{-1}$). This is the first example, in sulphur–nitrogen chemistry, of crystal growth by chemical transport. Well developed crystals of S_4N_3Cl also grew above the SO_2 level, but in the warmer ($35\,°C$) zone (*cf.* method 1). Although the $S_6N_4Cl_2$ crystals produced by this method showed nearly perfect rectangular facets on all sides, they adhered to the tube wall so strongly that it proved impossible to remove them without fracture. The identity of the S_4N_3Cl single crystals (up to 0.5 mm across), which separated easily from the wall, was established by a single-crystal precession photograph and a comparison with the known unit cell of this compound [13] [space group $P2_1/n$, $a = 19.29(2)$, $b = 10.46(1)$, $c = 9.36(1)$ Å, $\beta = 90.29°$, $Z = 12$].

Method 3. Preparation of Crystalline $S_6N_4Cl_2$ *by the Reaction of* $S_3N_2Cl_2$ *with Liquid* SO_2.—Finely ground $S_3N_2Cl_2$ was transferred in a glove box to a flask equipped with a Rotaflo valve and sulphur dioxide was condensed in (*ca.* 20 cm³ liquid SO_2 per gram of $S_3N_2Cl_2$). The dechlorination was almost complete (with occasional shaking) after *ca.* 5 d at room temperature; the reaction appeared to be catalyzed by sunlight.

After evaporation to dryness, the impure $S_6N_4Cl_2$ was transferred to the sealed extractor (Figure 1). Unreacted $S_3N_2Cl_2$ and by-product S_4N_3Cl were removed by SO_2 extraction (typically 15 cm³ SO_2, 0.3 g $S_3N_2Cl_2$, jacket cooled with tap water at $10\,°C$, flask at 25—$30\,°C$) until the fresh filtrate was colourless (*ca.* 2 h). The uniformly microcrystalline product (shiny green-black thin platelets, approx. 5 μm across) gave a well resolved X-ray powder diagram as shown in Table 1 (Found: Cl, 22.3; N, 17.7; S, 60.1. $S_6N_4Cl_2$ requires Cl, 22.2; N, 17.5; S, 60.2%).

(inside diameter 8 mm, length 140 mm) were prepared each containing purified $S_6N_4Cl_2$ (*ca.* 150 mg) and a mixture (total vol. *ca.* 8 cm³) of SO_2–$SOCl_2$: (a) 100 : 0, (b) 95 : 5, (c) 80 : 20, (d) 67 : 33, and (e) 0 : 100 v/v. A quartz e.s.r. tube (o.d. 4 mm) (f) was also prepared containing mixture (c). All tubes (a)—(f) were kept for 12 months with repeated temperature variations: 6 d in a freezer (T_1 *ca.* $-20\,°C$) and one day at room temperature (T_2 *ca.* $18\,°C$). Gradual increase in crystallite size of $S_6N_4Cl_2$ was clearly observable in ampoules (b)—(d) and (f). All the tubes were occasionally dipped (for *ca.* 3 min) in an ultrasonic bath to disperse crystal clusters. The best results were obtained with ampoule (c); well formed crystals of S_4N_3Cl appeared at the end of the warmer T_2 period, but during the cooling period (T_1) they disappeared completely and were replaced by numerous platelets of $S_6N_4Cl_2$ (up to 100 μm long) which nucleated on the tube wall.

In tubes (a) and (b), some S_4N_3Cl crystals remained on cooling and recrystallization was slow. In tube (e) the $S_6N_4Cl_2$ was unaffected; no S_4N_3Cl was formed during the entire 12-month period.

Raman spectra of the yellow supernatant solutions in all ampoules were examined at intervals and showed bands due to SO_2 and $SOCl_2$. Tubes (c) and (f) showed an extra unidentified weak band at 1 048 cm⁻¹.

At the end of the 12-month period no tubes showed an overpressure of nitrogen and tubes (c) and (f) provided a large number of well faceted approximately equidimensional crystals up to *ca.* 0.30 mm in length. The supernatant solution from tube (f) was decanted and pumped to dryness to give 10 mg of yellow crystals. I.r. spectra showed peaks due to S_4N_3Cl and five additional absorptions at 1 275s, 1 140m, 1 050m, 585w (sh), and 540w cm⁻¹ which could not be assigned to known sulphur–nitrogen compounds.

E.s.r. measurements. The supernatant SO_2–$SOCl_2$ solution in tube (f) gave a moderately strong e.s.r. spectrum near room temperature comprising a 1 : 2 : 3 : 2 : 1 quintet having a line spacing of 0.316 mT and a g factor of 2.01130 ± 0.00002.
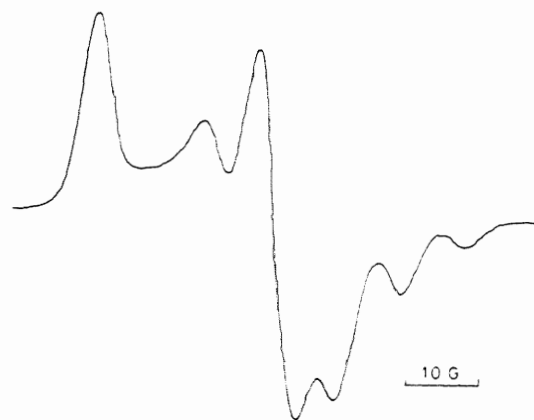
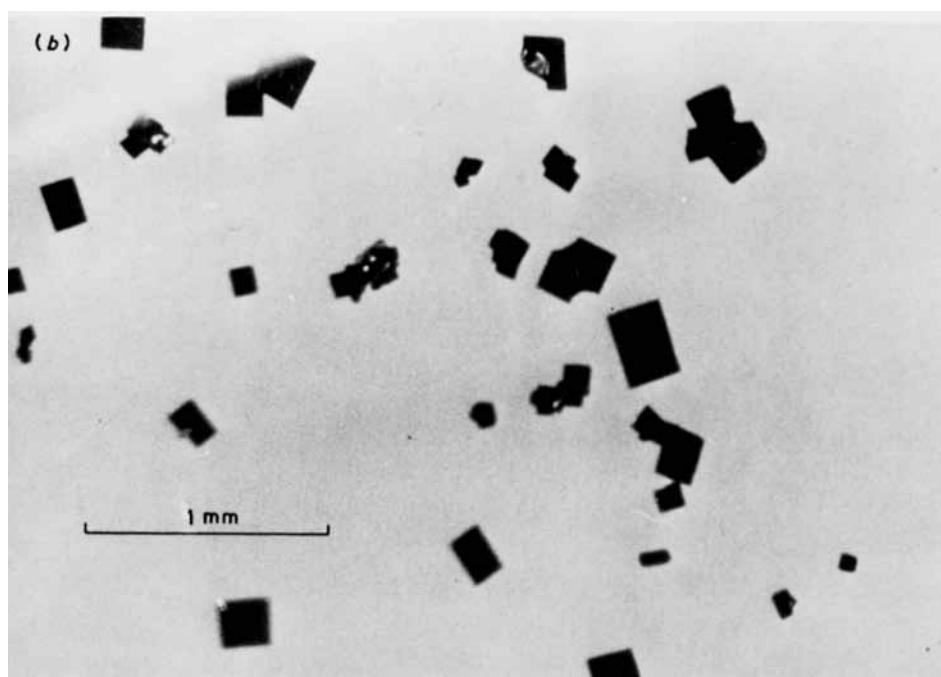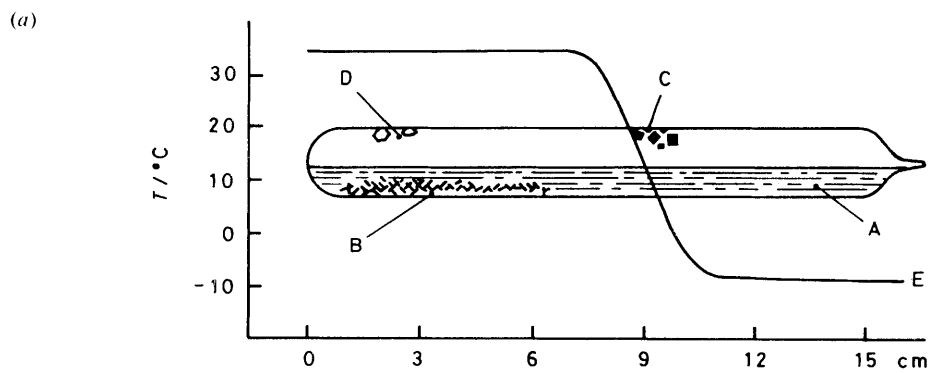**Figure 3.** (*a*) $S_6N_4Cl_2$ crystal growth (from $S_3N_2Cl_2$–SO_2) by chemical vapour transport in a sealed tube in a temperature gradient ($+35$ to -8 °C): A, liquid SO_2; B, $S_3N_2Cl_2$ *in situ* converted to $S_6N_4Cl_2$; C, growth site of $S_6N_4Cl_2$ crystals; D, S_4N_3Cl crystals; E, temperature profile along the tube. (*b*) Crystals of $S_6N_4Cl_2$ at site C photographed through the tube wall

Table 1. X-Ray powder diffraction data of $S_6N_4Cl_2$

Diffraction line no.	d_{hkl} (obs.)	d_{hkl} [a] (calc.)	h	k	l [a]	I/I_0 (obs.)	I/I_0 [b] (calc.)
1	7.290	7.230	0	2	0	w	11
2	5.317	5.286	1	1	1	vs	100
3	4.103	4.095	0	0	2	w	10
4	3.816	3.801	2	1	0	m	15
5	3.665	3.675	1	3	1	m	27
		3.633	1	0	2		
6	3.519	3.524	1	1	2	s	46
7	3.200	3.187	2	2	1	vs	78
8	3.058	3.050	2	3	0	s	27
9	2.857	2.859	2	3	1	s	43
		2.839	2	0	2		
10	2.792	2.786	2	1	2	m	10
11	2.659	2.664	2	4	0	s	53
		2.643	2	2	2		
12	2.559	2.563	1	4	2	s	30
		2.554	0	2	3		
13	2.176	2.178	0	4	3	m	5
14	2.066	2.057	0	6	2	m	12
15	1.888	1.886	3	4	2	m	10
		1.877	3	1	3		
16	1.675	1.677	3	4	3	m	8
		1.666	4	3	2		
17	1.519	1.513	5	2	1	m	8
		1.513	4	5	2		
18	1.404	1.408	2	8	3	m	8
19	1.150	1.152	2	12	0	w	1
20	0.869	—	—	—	—	w	—

[a] The unit-cell parameters of $S_6N_4Cl_2$ were used as input data for a computer program to generate indexed d_{hkl} values (D. A. Appleman and H. T. Evans, jun., 'Indexing and Least Squares Refinement of Powder Diffraction Data,' U.S. Geological Survey, Geologic Division, Washington D.C., 1973). [b] The relative intensities were calculated from structure factor data obtained in this work. For diffraction lines overlapping (within the error in measurement) the relative intensity data are given as a sum for the two sets of hkl.

Table 2. Fractional atomic co-ordinates ($\times 10^4$) with estimated standard deviations (e.s.d.s.) in parentheses

Atom	x	y	z
S(1)	−136(2)	2 777(1)	8 950(2)
S(2)	499(2)	4 564(1)	7 964(2)
S(3)	1 739(2)	4 216(1)	10 193(2)
N(1)	1 104(6)	3 152(3)	10 284(6)
N(2)	−398(6)	3 554(3)	7 657(6)
Cl	2 695(2)	6 003(1)	9 022(2)

of the usual green-black form given in Table 1) and from the i.r. spectrum: 1 018m, 962s, 944s, 707vs, 698vs, 585s, 433s, and 371s cm⁻¹. The two forms are both stable in dry air.

Crystal Structure of $S_6N_4Cl_2$.—*Crystal data.* $S_6N_4Cl_2$, orthorhombic, space group $Pbca$, $a = 7.88(1)$, $b = 14.46(1)$, $c = 8.19(1)$ Å, $U = 933.2$ Å³, $Z = 4$, $D_c = 2.27$ Mg m⁻³, $F(000) = 632$, $\lambda(\text{Mo-}K_\alpha) = 0.7107$ Å, $\mu = 1.842$ mm⁻¹. Intensity data from a crystal of dimensions 0.35 × 0.007 × 0.30 mm were collected for the layers $l = 0$—9 on a Stoe STADI-2 automatic two circle diffractometer using graphite-mono-chromatised Mo-K_α radiation. Absorption corrections were applied to the 792 unique measured reflections; of these, 563 having $I > 3\sigma(I)$ were retained for refinement of the structure. All calculations were carried out with the SHELX [14] suite of programs.

Structure determination. A model of the structure was obtained by the use of the direct-methods program EEES of the SHELX suite. Positional and anisotropic thermal para-meters for all six atoms were refined by full-matrix least squares. At a later stage individual scale factors for the data collection layers were refined. When the parameter shifts were all less than 10⁻³ of the corresponding e.s.d., R was 0.031 and the refinement was terminated. Atomic scattering factors were taken from ref. 15. The final atomic co-ordinates are given in Table 2.

Structural data. The structure and dimensions are shown in Figure 4 and in Table 3. As found for the chlorodisulphate,[1] the two parallel S_3N_2 rings are planar [10] to within one e.s.d. (0.02 Å) and are joined by weak S⁻ bonds to form a centro-symmetric tricyclic dimer. The dihedral angle between the plane of the S_3N_2 ring and that of the S_4 ring is 110.4(3)° [109.4(2)° in the $ClS_2O_6^-$ salt; this angle was calculated from atomic co-ordinates given in ref. 16].

Crystals large enough for the X-ray structure determination were obtained from $S_3N_2Cl_2$ by a controlled extraction with sulphur dioxide as follows. With unground $S_3N_2Cl_2$ (0.35 g) on the frit [Figure 1, C] at 0 °C and liquid SO_2 at 15 °C in the flask (protected from sunlight), there was a steady flow of weak $S_3N_2Cl_2$ solution into the flask; the solubility of $S_3N_2Cl_2$ in SO_2 is very low. After 14 d, the extent of reaction was *ca.* 50%. The platelets of $S_6N_4Cl_2$ on the frit were mixed with unreacted $S_3N_2Cl_2$ but the flask contained numerous well formed thin (*ca.* 2 μm, and up to *ca.* 1 mm wide) transparent (red) platelets of $S_6N_4Cl_2$, a few of which were thick enough (*ca.* 10 μm) to be handled. These crystals gave clear diffraction spots (better resolved than for crystals from method 1) and so were used for the structure determination.

Method 4. The Red Form of $S_6N_4Cl_2$.—Cyanamide, $NCNH_2$ (0.042 g, 1 mmol) was added gradually to powdered $S_3N_2Cl_2$ (0.195 g, 1 mmol) in an agate mortar, with grinding after each addition. The heat of reaction caused melting of the cyanamide to give a rusty brown paste; this crystallized on standing (several hours). Grinding then gave a dark brown powder. No gas was evolved during the reaction. I.r. absorptions (Nujol mull) were observed at 3 180m, 2 160vs, 1 695vs, 1 171s, 913m, 791vs, 669s, 482s, 382vs, 350s, 283s, 170vs, 138s, and 90m cm⁻¹; m.p. 91 °C (with decomposition to a red-brown liquid).

The adduct rapidly decomposed in liquid SO_2 (at −3 °C) to give a carmine red precipitate which was identified as pure $S_6N_4Cl_2$ from the X-ray powder diagram (identical with that

Results and Discussion

The initial experiments in this study arose from the observation [12] that solutions of S_4N_3Cl in $SOCl_2$, when cooled below *ca.* −5 °C deposited not only yellow S_4N_3Cl but also green-black $S_6N_4Cl_2$. The very small $S_6N_4Cl_2$ crystals that formed (and the green inclusions in the S_4N_3Cl crystals) disappeared on warming. The solutions remained yellow throughout the process. This interconversion was also observed in pure SO_2 during solvent extraction of crude $S_6N_4Cl_2$ (see Experimental section) hence leading to preparation method 2.

1. *Sealed Tube Recrystallisation of* $S_6N_4Cl_2$ *suspended in* SO_2-$SOCl_2$.—These experiments confirmed the remarkably facile interconversions of S_4N_3Cl and $S_6N_4Cl_2$, and helped to indicate suitable conditions for crystal growth of $S_6N_4Cl_2$ in method 2.

2. *Growth of* $S_6N_4Cl_2$ *Crystals by Vapour Transport.*—In this method (sealed tube of $S_3N_2Cl_2$-liquid SO_2 placed in a

Figure 4. The $S_6N_4Cl_2$ molecule, with distances (Å) and angles (°)

temperature gradient of $+35$ to $-8\ °C$), $S_6N_4Cl_2$ and S_4N_3Cl crystals were formed within a film of liquid SO_2 on the upper side of the horizontal reaction tube (Figure 3). Since they are practically involatile at the maximum temperature of the reaction tube (35 °C), we concluded that their crystal growth occurred as a result of a chemical transport reaction *via* some volatile covalent intermediate(s) present in low concentration, probably detected in (*i*) the Raman spectra of solutions (one extra band at 1 048 cm^{-1}) and/or (*ii*) i.r. spectra of dry residues (*ca.* five additional i.r. bands). Possible intermediates are S=N–SCl, O_2S=N–SCl, S–S–N=S=N, or O_2S–S–N=S=N, all of which are unknown. Equilibria involving other undetected volatiles are also likely [*e.g.* as in equations (1) and

$$S_4N_4 + S_2Cl_2 \qquad (1)$$

$$3\ S_4N_4 + 2\ S_2Cl_2 \rightleftharpoons 4\ S_4N_3Cl \qquad (2)$$

(2)]. Reaction (2) is known.[17] The free-radical monomer S_3N_2Cl (detected by the e.s.r. method) was also present.

Since S_4N_3Cl has shorter mean $d(SN)$ (1.555 Å), shorter $d(SS)$ (2.078 Å) and also less strained ring angles than $S_6N_4Cl_2$ (see section 4 below), it is curious that this stable species decomposes to $S_6N_4Cl_2$ on *cooling*. Several reasons are possible: perhaps $S_6N_4Cl_2$ dissociates on warming to produce, in addition to S_4N_3Cl, some other stable species which may then react with the solvent (thus supporting the above discussion of possible reactions).

In both methods 1 and 2 for preparing crystalline $S_6N_4Cl_2$, the formation of $S_6N_4Cl_2$ (rather than S_4N_3Cl) required temperatures below *ca.* 5 °C. Crystallite growth from solution due to fluctuating temperature is well known; the driving force for the process is the minimization of surface free energy, ΔG_s. But the difference in our case is that the dissolution–precipitation cycle is accompanied by chemical reaction.

3. *Preparation of Crystalline* $S_6N_4Cl_2$ *from* $S_3N_2Cl_2$–SO_2.— As described above (method 2) and in agreement with Vincent *et al.*[10] we observed that liquid SO_2 dechlorinates $S_3N_2Cl_2$ at room temperature: equation (3). When the impure product is

$$2\ S_3N_2Cl_2 + SO_2 \longrightarrow S_6N_4Cl_2 + SO_2Cl_2 \qquad (3)$$

removed and extracted with further liquid SO_2, the reaction goes to completion, contaminants (principally S_4N_3Cl) are removed and the method provides a very simple and convenient preparation of $S_6N_4Cl_2$. The purity is superior to that obtained by other methods,[11] the product is crystalline (typically 5 μm wide, thin microcrystals) and the yield [*ca.* 85% based on equation (3)] is high. In comparison, the theoretical yield by the standard method [9] (vacuum decomposition of $S_3N_2Cl_2$) is 67%: equation (4).

$$3\ S_3N_2Cl_2 \xrightarrow{ca.\ 85\ °C} S_6N_4Cl_2 + 2\ NSCl \pm SCl_2 \qquad (4)$$

Green-black $S_6N_4Cl_2$ leaves a carmine red trace when rubbed on paper.[11] The red form of $S_6N_4Cl_2$ obtained by method 4 is an identical colour. A similar carmine deposit (presumably $S_6N_4Cl_2$) is formed on the walls when a glow discharge (*e.g.* as generated by a high frequency spark tester) acts on $S_3N_2Cl_2$ in an evacuated vessel.

4. *Structure and Bonding in* $S_6N_4Cl_2$.—The S–N ring distances in the cation [$d(SN) = 1.557$—1.642 Å] are the longest where adjacent to the SS bond, which is consistent

Table 3. Bond distances (Å) and angles (°) for $S_6N_4Cl_2$ compared with those for $[S_6N_4][ClS_2O_6]_2$[1,16]

(a) Distances	$S_6N_4Cl_2$	$[S_6N_4][ClS_2O_6]_2$		(b) Angles	$S_6N_4Cl_2$	$[S_6N_4][ClS_2O_6]_2$
S(1)–N(1)	1.563(5)	1.563(3)		N(1)–S(1)–N(2)	107.9(2)	107.6(2)
S(1)–N(2)	1.557(5)	1.574(3)		S(1)–N(2)–S(2)	118.7(3)	119.1(2)
N(1)–S(3)	1.618(4)	1.609(3)		S(1)–N(1)–S(3)	119.4(3)	119.55(20)
N(2)–S(2)	1.642(4)	1.601(3)		N(2)–S(2)–S(3)	96.8(2)	97.2(2)
S(2)–S(3)	2.131(2)	2.145(1)		N(1)–S(3)–S(2)	97.0(2)	96.6(2)
S(2)–S(3ᴵ)	2.916(2)	3.027(1)				
Cl–S(2)	2.842(2)					
Cl–S(3)	2.858(2)			Symmetry codes		
Cl–S(1ᴵ)	3.152(2)			Superscript I: $-x, 1 - y, 2 - z$		
Cl–S(1ᴵᴵ)	3.207(2)			Superscript II: $\frac{1}{2} - x, \frac{1}{2} - y, z$		
Cl–S(3ᴵᴵᴵ)	3.184(2)			Superscript III: $\frac{1}{2} - x, 1 - y, z - \frac{1}{2}$		

with valence bond canonical structures of the form shown below.
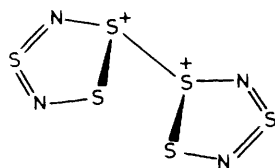
Within the S_3N_2 rings, the SS and SN distances [d(SS) = 2.131(2), d(SN) = 1.557(5)—1.642(4) Å] are typical of S_3N_2 ring systems [in which d(SS) and mean d(SN) have been found [18] to vary: d(SS) = 2.13—2.23 Å and d(SN) = 1.58—1.61 Å].

Compared with the $ClS_2O_6^-$ salt (Table 3), the SS bonds (within and between the S_3N_2 rings) are slightly stronger and the adjacent SN bonds are slightly weaker. An analogous situation occurs for the chloride and tetrachloroferrate(III) salts of $S_3N_2Cl^+$: the larger charge transfer from Cl⁻ (compared with $FeCl_4^-$) again strengthens (by 0.045 Å) [18] the sulphur–sulphur link in the S_3N_2 ring.

The bond angles all betray some compression due to constraint within a small ring. Correlations [19] between bond distances (pm) and bond angles (°) for unstrained and largely unstrained sulphur–nitrogen compounds [*viz.* d(NS) = $177.47 - 0.1421\overset{\frown}{N}$ (angle at nitrogen) and d(SN) = $213.14 - 0.4816\overset{\frown}{S}$ (angle at sulphur) pm] indicate compressions of the order of 10° at both N and S (*cf.* the S_3N_2 ring in $S_3N_2Cl^+$).[20] This situation contrasts with that for S_4N_3Cl which has wider and largely unstrained angles [NSN = 118.1—119.5(2)° and SNS = 135.0—135.9(2) or 150.4—152.4(3)°] and has a shorter mean d(SN) (1.555 Å).[13]

The chloride 'ions' in $S_6N_4Cl_2$ contact only sulphur atoms. van der Waals radii for sulphur and for the chloride ion are both *ca.* 1.8 Å and the contact distances are all below 3.6 Å: two at 2.84—2.86 Å and three at 3.15—3.21 Å (Table 3). Similar S–Cl distances were found [20] for $[S_3N_2Cl][FeCl_4]$ (two close to 2.85 Å and two at 3.14—3.22 Å) and for S_4N_3 [2.808(2) and 2.921(2) Å to the disulphide sulphurs].[13] In $S_6N_4Cl_2$, one of the effects of weak S···Cl bonding (at > 2.86 Å) is a 0.29(2) Å displacement of Cl⁻ from the plane of the nearer S_3N_2 ring away from the neighbouring S_3N_2 ring.

The similar distances between Cl and S(1ᴵ), S(1ᴵᴵ), and

S(3ᴵᴵᴵ) probably represent an equilibrium value for a weak residual ionic effect, while the shorter S(2)–Cl and S(3)–Cl distances include an additional covalent contribution. The compound is therefore not strictly a dimeric dithiadiazolium salt, hence the choice of the trivial name hexasulphur tetranitrogen dichloride.

References

1 A. J. Banister, H. G. Clarke, I. Rayment, and H. M. M. Shearer, *Inorg. Nucl. Chem. Lett.*, 1974, **10**, 647.
2 M. Becke-Goehring, *Prog. Inorg. Chem.*, 1959, **1**, 221.
3 O. Glemser, *Angew. Chem., Int. Ed. Engl.*, 1963, **2**, 530.
4 R. J. Gillespie, J. P. Kent, and J. F. Sawyer, *Inorg. Chem.*, 1981, **20**, 3784.
5 H. W. Roesky and A. Hamza, *Angew. Chem., Int. Ed. Engl.*, 1976, **15**, 226.
6 R. J. Gillespie, P. R. Ireland, and J. E. Vekris, *Can. J. Chem.*, 1975, **53**, 3147.
7 L. Friedman and P. Wetter, *J. Chem. Soc. A*, 1967, 36.
8 W. L. Jolly and K. D. Maguire, *Inorg. Synth.*, 1967, **9**, 106.
9 W. L. Jolly and K. D. Maguire, *Inorg. Synth.*, 1967, **9**, 109.
10 H. Vincent, Y. Monteil, and M. P. Berthet, *Z. Anorg. Allg. Chem.*, 1980, **471**, 233.
11 H. G. Heal, 'The Inorganic Heterocyclic Chemistry of Sulfur, Nitrogen and Phosphorus,' Academic Press, London, 1980, pp. 121—122.
12 A. J. Banister and Z. V. Hauptman, *J. Chem. Soc., Dalton Trans.*, 1980, 731.
13 B E Svenningsen and R G. Hazell, personal communication.
14 G. M. Sheldrick, SHELX 76, program for crystal structure determination, University of Cambridge, 1976.
15 D. T. Cromar and J. B. Mann, *Acta Crystallogr., Sect. A*, 1968, **24**, 321.
16 I. Rayment, Ph.D. Thesis, University of Durham, 1975.
17 M. Goehring, *Sci. Chim.*, 1957, **9**, 75.
18 G. K. Maclean, J. Passmore, and P. S. White, *J. Chem. Soc., Dalton Trans.*, 1984, 211.
19 A. J. Banister and J. A. Durrant, *J. Chem. Res.*, 1978, (*M*) 1910, 1928.
20 H. M. M. Shearer, A. J. Banister, J. Halfpenny, and G. Whitehead, *Polyhedron*, 1983, **2**, 149.